3 Biotech (2023) 13:227
https://doi.org/10.1007/s13205-023-03646-4

ORIGINAL ARTICLE

# Defensin-based therapeutic peptide design in attenuating V30M TTR-induced Familial Amyloid Polyneuropathy

G. Chandrasekhar[1] · H. Pengyong[2] · G. Pravallika[1] · L. Hailei[2] · X. Caixia[2] · R. Rajasekaran[1]

Received: 22 December 2022 / Accepted: 24 May 2023 / Published online: 8 June 2023


## Abstract

In the present study, we aimed to formulate an effective therapeutic candidate against V30M mutant transthyretin (TTR) protein to hinder its pathogenic misfolding. Nicotiana alata Defensin 1 (NaD1) Antimicrobial Peptide (AMP) was availed due to its tendency to aggregate, which may compete for aggregation-prone regions of pathogenic TTR protein. Based on NaD1's potential to bind to V30M TTR, we proposed NaD1-derived tetra peptides: CKTE and SKIL to be initial therapeutic candidates. Based on their association with mutant TTR protein, CKTE tetra peptide showed considerable interaction and curative potential as compared to SKIL tetra peptide. Further analyses from discrete molecular dynamics simulation corroborate CKTE tetra peptide's effectiveness as a 'beta-sheet breaker' against V30M TTR. Various post-simulation trajectory analyses suggested that CKTE tetra peptide alters the structural dynamics of pathogenic V30M TTR protein, thereby potentially attenuating its beta-sheets and impeding its aggregation. Normal mode analysis simulation corroborated that V30M TTR conformation is altered upon its interaction with CKTE peptide. Moreover, simulated thermal denaturation findings suggested that CKTE-V30M TTR complex is more susceptible to simulated denaturation, relative to pathogenic V30M TTR; further substantiating CKTE peptide's potential to alter V30M TTR's pathogenic conformation. Moreover, the residual frustration analysis augmented CKTE tetra peptide's proclivity in reorienting the conformation of V30M TTR. Therefore, we predicted that the tetra peptide, CKTE could be a promising therapeutic candidate in mitigating the amyloidogenic detrimental effects of V30M TTR-mediated familial amyloid polyneuropathy (FAP).

**Keywords** Familial amyloid polyneuropathy · Protein aggregation · Peptide-based therapeutics · Discrete molecular dynamics · Normal mode analysis

## Introduction

Transthyretin-mediated familial amyloid polyneuropathy (TTR FAP) is a debilitative autosomal dominant neuropathic genetic disorder, most frequently caused by valine to methionine pathogenic substitution at the 30th position of transthyretin protein. It is peculiarized by aberrant aggregation and deposition of misfolded amyloid forms of TTR protein in vital areas including the heart, autonomic and peripheral nervous system, kidneys, eyes, and other pertinent areas. And, it is frequently predominated by progressive and tenacious nerve damage including autonomic axonal and sensorimotor polyneuropathy, which often exhibits multi-systemic manifestations. Also, restrictive cardiomyopathies that entail rhythm disturbance and conduction blocks are associated with TTR FAP. Ocular impairment and renal complications have also been observed; but less frequent. Regardless, the pathological ramifications could result in progressive organ failure and are even, considered life-threatening in certain situations (Bonaïti et al. 2010; Ando et al. 2013; Rowczenio et al. 2014; Santos et al. 2015; Sekijima 2015; Conceição et al. 2016; Sekijima et al. 2018; Srinivasan et al. 2020).

G. Chandrasekhar and H. Pengyong are contributed equally to this work.

✉ X. Caixia
caixia@czmc.edu.cn

✉ R. Rajasekaran
rrajasekaran@vit.ac.in

[1] Quantitative Biology Lab, Department of Integrative Biology, School of Bio Sciences and Technology, Vellore Institute of Technology (VIT, Deemed to Be University), Vellore, Tamil Nadu 632014, India

[2] Changzhi Medical College, Changzhi 046000, China

The liable biomolecular agent behind this detrimental disorder is Transthyretin (TTR), a 55 kDa homo-tetramer protein that is found predominantly in cerebrospinal fluid and blood plasma. Synthesized in the liver, it is responsible for carrying thyroxine in cerebrospinal fluid and transporting both thyroxine and vitamin A to the liver. Each monomer of TTR comprises 127 amino acids and the structural changes induced by pathogenic point mutations, cause TTR tetramers to dissociate and misfold into amyloid fibrils, which are typically rich in beta-sheets and resilient to proteasomal degradation. Moreover, the aggregation and the accumulation of amyloid fibrils in tissues ensues cyto-degeneration and eventually, organ failure. Among the pathogenic point mutations, V30M is most predominantly observed in TTR FAP patients, with endemic foci to Swedish, Japanese and Portuguese populations; that can afflict several detrimental effects in patients (Saraiva 1995; Arvidsson et al. 2015; Gertz et al. 2015; Sharma et al. 2019).

Till now, liver transplantation has remained the standard therapeutic strategy against TTR FAP. Though effective, it is known to distress patients with unprecedented side effects and in certain cases, the pathogenic effects remain persistent (Adams 2013; Carvalho et al. 2015; Gertz et al. 2015). Furthermore, tafamidis, a pharmaco-therapeutic with adverse side effects such as punctate keratitis, nasopharyngitis, upper respiratory tract infection, etc. (Coelho et al. 2013) is prescribed against TTR FAP for its ability in regulating TTR aggregation. Hence, an effective curative strategy against this lethal disorder is necessitated.

Fortunately, peptide-based therapeutics is being increasingly hypothesized for its role in alleviating the cytotoxic amyloidogenic proteins. In fact, the potent peptide-based bio-molecular strategies to therapeutically intervene with proteopathic protein misfolding into their amyloid form have been quite effective (Baig et al. 2018; Armiento et al. 2020). Among these strategies, the repurposing of antimicrobial peptides, especially defensins against aggregation-prone proteins, is quite promising. Findings indicated that defensins demonstrate an enhanced binding with amyloid aggregates, to suppress the residual interactions imperative for self-aggregation. A study conducted by Tang et al., suggested that human $\beta$-defensin 1 (HBD-1) and human $\alpha$-defensin 6 (HD-6) can interact with Aβ (associated with Alzheimer's), hCT (associated with medullary thyroid carcinoma) and hIAPP (associated with type II diabetes) to impede their aggregation towards amyloid formation. Similarly, Zhang et al. reported that α-defensins containing $\beta$-rich structures are able to interact with amyloidogenic proteins Aβ, hCT and hIAPP to prevent its pathogenic misfolding and aggregation (Zhang et al. 2021; Tang et al. 2022).

Among the defensins, the anti-microbial peptide (AMP) Nicotiana alata Defensin 1 (NaD1) exhibits a notable potency against fungi due to its self-aggregation property that aids in microbial membrane infiltration (van der Weerden et al. 2008, 2010; Hayes et al. 2018; Järvå et al. 2018). This self-aggregation propensity of NaD1 could possibly mimic aggregation-prone hotspots of aberrant proteins and effectively re-alter the conformational dynamics to impede their pathogenic transformation into amyloid form.

Significantly, the computational advancements in the field of molecular modelling and drug design have enabled researchers to assess the curative effects of lead compounds against pathogenic proteins, prior to experimental validation, which has notably reduced the number of potent molecules to be tested in vitro, thereby considerably saving resources and time. Several in silico analyses elucidating the biochemical dynamics between lead compounds and aberrant pathogenic proteins, especially the ones that are aggregation-prone, have been efficiently carried out in the recent past (Lemkul and Bevan 2012; Hassan et al. 2018; Jakubowski et al. 2020; Srinivasan et al. 2022).

In the present analysis, with the help of proficient molecular modelling tools and pipelines, we have rationally designed therapeutic peptides from plant defensin antimicrobial peptide (AMP) Nad1 and assessed their curative potential against V30M TTR protein. Our aim is to contrive a shorter, yet potent peptide that could effectively interact with V30M mutant TTR protein and notably re-alter its pathogenic architecture to negate the aberrant misfolding into an amyloid form. Herein, tackling the problem head-on at its source itself could effectually prevent the aberrant accumulation of TTR aggregates in crucial organs.

## Materials and methods

### Structural coordinates optimization

Initially, the 3D structural coordinates of pathogenic V30M TTR (ID: 4TL4) protein and NaD1AMP (ID: 1MR4) were retrieved from the PDB database (Lay et al. 2003; Saelices et al. 2015). Both the protein and peptide's geometry were optimized, by subjecting their structural coordinates to the steepest descent algorithm through YASARA software, an adept tool for molecular modelling, visualization, and simulation. The optimized structure of protein and peptide was utilized for further analysis.

### Molecular docking

To ascertain the association between peptide and mutant TTR protein, Cluspro molecular docking tool was employed, which is an efficient server for ascertaining protein–protein interaction. Initially, the protein structures are optimized prior to docking by Cluspro. Several possible conformations of ligand/peptide are generated and then, the rigid

body docking is performed with the afore-generated ligand conformers and protein. Herein, the tool employs the PIPER docking program to ascertain the interactions between protein and ligand. It employs a more accurate scoring function that also computes desolvation parameters and electrostatic interactions. Based on the docking scores, the top 1000 complexes are shortlisted and then based on their conformational orientation, they are clustered further. Finally, a post-docking conformational refinement is performed on the resultant structures, and the complex model from the largest cluster with the highest docking score is selected for further analysis (Kozakov et al. 2017; Vajda et al. 2017). Furthermore, the mutant V30M TTR protein active site residual binding energy with peptides is ascertained with the help of MM/GBSA analysis performed by the Hawk Dock server(Weng et al. 2019).

## HOMO–LUMO energy gap computation

To further elucidate the chemical reactivity of therapeutic peptides with mutant TTR, the highest occupied molecular orbital (HOMO)–lowest unoccupied molecular orbital (LUMO) energy gaps of the peptide molecules were computed, upon docking with V30M TTR protein. In brief, the computations were performed with AMPAC software (http://www.semichem.com/ampac/default.php), a proficient semi-empirical quantum mechanical molecular modelling program. Besides, the molecular orbital parameters of peptides were ascertained quantum semi-empirically, with the help of parameterizations stipulated by the PM6 model (Stewart 2007). Subsequently, the HOMO–LUMO energy gaps were calculated for the peptide molecules.

## Steered molecular dynamics (SMD) simulation

SMD simulation was performed on the peptide complexes with mutant TTR, using YASARA molecular modelling software, based on the parameterizations of the AMBER force field. Initially, the simulation system is solvated with 0.997 g/ml solvent density water molecules, and the temperature is maintained at 298 K. Further, the charge of system is neutralized by adding 0.9% sodium chloride. Also, the long-range coulomb interactions were incorporated with periodic boundary conditions (PBC). Further, the peptide candidates are systematically pulled from mutant TTR with a dynamic pulling acceleration of 1500 pm/picosecond$^2$. During the simulation, the centre mass of V30M mutant TTR is maintained constant, while the peptides are pulled from it, systematically. Also, the simulation parameters are recorded, once every 10 picoseconds. The simulation concludes, when the peptides get completely dissociated from their respective complex with mutant V30M TTR, at a 25 Å distance. The peptide that showed a notable interaction with mutant TTR was utilized for subsequent analysis (Srinivasan and Rajasekaran 2019a; Srinivasan et al. 2021a).

## Discrete molecular dynamics (DMD) simulation

Besides, the dynamic association between the selected therapeutic peptide and V30M TTR was elucidated with the help of DMD simulation. DMD is a modified version of classical MD simulation, in which the biomolecular trajectory depicts a discrete set of events, rather than continuous, making DMD relatively faster, yet as effective as classical MD. DMD performs event-driven ballistic motion-based computations to ascertain atomic displacements. Also, the Medusa force field is incorporated into the pipeline to parameterize the molecular interactions. Notably, the Medusa force field is used to effectively study protein folding and the structural pathogenic perturbations induced by mutations. Besides, DMD simulation is quite apt for studying the structural dynamics of amyloidogenic proteins(Dokholyan et al. 1998; Shirvanyants et al. 2012). To represent the protein structures, a united-atom model is used. Further, Lazaridis Karplus implicit solvation model is utilized, by the simulation system to account for protein structure solvation (Lazaridis and Karplus 1999). And, the molecular H-bond interactions are computed with the help of the Reaction-like algorithm (Ding et al. 2008). Further, the inter-atomic charge interactions are ascertained with the help of the Debye-Hu¨ckel approximation, wherein the Debye length is restricted to 10 Å. Also, the temperature is regulated and maintained at 300 K using Andersen's thermostat (Andersen 1980) and the PBC are effectuated during the simulation. Subsequently, the dynamic molecular configurations of the protein structures are recorded once in every 100-time units (tu), and the entire simulation was carried out, for 1,00,000 tu. Post simulation, the dynamic changes in secondary structural propensities of the protein structures were determined with the help of Dictionary of Secondary Structure of Proteins (DSSP) algorithm. Moreover, DMD simulation trajectory analyses were carried out, using GROMACS package (Van Der Spoel et al. 2005). Upon simulation, the difference between molecular trajectories of V30M TTR protein and its complex with therapeutic candidate peptide are statistically substantiated, by performing a nonparametric Wilcoxon test on their trajectory dataset, with the help of Python's Scipy package (version 1.6.2).

## Normal mode analysis (NMA)

To further elucidate the dynamic interaction between the selected therapeutic peptide and V30M TTR protein, NMA simulation was performed on the protein structures. NMA is a computational pipeline that elucidates the conformational dynamics of a system based on its harmonic motion. NMA

is typically used to ascertain larger time-scale conformational transitions of protein structures that are quintessentially laborious for MD simulations. Herein, the dynamic conformational change is elucidated by the superposition of normal modes and their corresponding frequencies (Go et al. 1983; Levitt et al. 1985; Hinsen 1998; Bahar et al. 2010). First, the DynaMut server was used to compute the residual deformation potential of V30M TTR and its complex with the peptide. It effectively ascertains conformational changes of protein structure based on principles of NMA and based on Amber94 all-atom potential parameterizations. Subsequently, an inter-residual apparent stiffness was computed for the protein structures with the help of the FlexServ server, which employs a vectorial Anisotropic Network Model (ANM) NMA formalism to ascertain the conformational dynamics of protein structures. With the help of a diagonalized hessian matrix, the ANM formulates eigenvectors and eigenvalues that in turn delineate shape, frequencies and directions of normal modes (Camps et al. 2009; Rodrigues et al. 2018).

### Frustrometer analysis

To evaluate V30M TTR protein structural integrity upon its binding with the selected therapeutic peptide, the Frustrometer tool was used to assess the protein structure residual frustration/strain. The tool determines the residual frustration of queried protein, based on the energy landscape theory. It computes the likelihood that a given amino acid will conformationally reorient, based on the structural strain, it experiences from the surrounding residues (restricted to a 5 Å sphere around each Cα). Specifically, the frustration elucidated by each residue is calculated based on a probabilistic model, wherein the current position of a given residue is compared against the same residue's all possible conformational positions in the given vicinity. Subsequently, the resultant change in energy was measured, according to parameters specified by the AMW energy function. Also, the amino acids can be categorized as minimally frustrated, neutral or highly frustrated, based on the computed normalized *Z*-score. Accordingly, a residue is said to be 'minimally' frustrated, if the elucidated *Z*-score is higher than 0.78, while it is 'highly frustrated' if the *Z*-score is lower than −0.78 and the scores in-between are delineated as neutral (Dixit and Verkhivker 2011; Parra et al. 2016).

### Simulated thermal denaturation

To further investigate the structural influence of the selected peptide on V30M TTR, the simulated thermal denaturation of protein structures was performed, using Proflex software. It uses the Pebble game algorithm, and models the interactions such as hydrophobic, polar, H-bonds and covalent bonds, during simulation. Based on the structural geometry of the queried protein, it is demarcated into flexible and rigid regions. Then, the H-bonds of the protein structure are removed systematically from weakest to strongest, till the protein is completely denatured/unfolded. After each cycle of H-bond removal, the protein's structural geometry is recalibrated and subsequently demarcated into rigid and flexible regions. Next, the energy required for H-bond removal is recorded. While doing so, the energy required to remove the H-bonds is ascertained with the help of the Mayo potential. Also, the energy cut-off parameter for simulation is set to −1.0 kcal/mol, for H-bond removal (Rader et al. 2002; Srinivasan and Rajasekaran 2017).

## Results and discussion

Amyloidogenic disorders have distressed mankind for a longer period of time. Yet, their pathophysiological mechanisms are largely obscure. Moreover, formulating an efficient therapeutic strategy against these detrimental disorders has been a herculean task. Furthermore, while much importance is given to disorders such as Alzheimer's, Parkinson's, ALS and Huntington, an equally debilitative FAP disorder is comparatively unheeded. Among FAP patients, V30M mutation in TTR protein is found to be the most common genetic aberration. This point mutation in TTR propagates it to misfold into amyloids, which further promotes cellular degeneration in the tissues where it gets aggregated (Saraiva 1995; Srinivasan et al. 2020). In the current analysis, we intended to formulate therapeutics that could effectively alter the conformation of V30M TTR protein and steer it away from its distinct pathogenic tendency to misfold into amyloid fibrils, thereby addressing the source of the predicament to effectively prevent aggregation in crucial regions.

Recently, peptide-based therapeutics has begun to gain a lot of traction for their efficacy against amyloidogenic disorders. Compared to small molecules, the peptide-based therapeutics exhibit higher potency and specificity, thus lower toxicity. And, they are relatively easier to synthesise when compared to small molecules. Moreover, they elicit low immunogenic responses relative to small molecules (La Manna et al. 2018; Wang et al. 2022). A study conducted by Wang et al. (2011) suggested that a therapeutic peptide candidate molecule designed was able to mitigate Aβ aggregation and its subsequent neuronal damage. Also, Cheruvara et al. (2015) suggested that the candidate peptide molecule, 4554W instigated a decrease in α-synuclein fibril formation and a reduction in cytotoxicity. And, Soto et al. reported short beta-sheet breaker peptides which were able to impede Aβ fibrillogenesis. Similarly, several studies have reported that peptide-based analeptics have attenuated the cytotoxic propensities of various detrimental amyloidogenic

proteins (Armiento et al. 2020). Although peptide-based therapeutics are susceptible to proteolysis, recent peptide modification advancements such as hydrocarbon stapling or substituting residues with non-natural amino acids could potentially evade its proteolytic cleavage. Recent progress in drug delivery routes and chemical medication reactions could circumvent the potential shortcomings associated with peptide-based curative, making them efficacious (Werle and Bernkop-Schnürch 2006; Walensky and Bird 2014; Baig et al. 2018; La Manna et al. 2018).

Especially, defensins have been known to exhibit a preferential interaction with amyloid fibrils to mitigate its detrimental effects(Zhang et al. 2021; Tang et al. 2022). Among these, NaD1 defensin, a potent anti-fungal peptide found predominantly in ornamental tobacco plants could be a prudent choice in targeting V30M TTR pathogenic protein. The rationale for choosing this particular AMP is that it is known to self-aggregate (van der Weerden et al. 2010; Hayes et al. 2018; Järvå et al. 2018). It is highly plausible that the residues from this aggregation-prone AMP may complement the aggregation-prone regions of pathogenic V30M TTR protein. Thus, it is also likely that the aforementioned amino acids from NaD1 AMP could notably interact with V30M TTR protein and alter its pathogenic conformational dynamics, to mitigate its conventional amyloidogenic misfolding. Based on these postulations, we attempted to formulate NaD1 AMP-based therapeutic peptide candidate against V30M TTR protein, to potentially alter its distinct pathogenic structural dynamics.

## Elucidating key residues involved in NaD1 interaction with V30M TTR protein

NaD1 is a 47-residue-long AMP peptide, however, shorter peptides have been found to be therapeutically favourable compared to their longer counterparts (Apostolopoulos et al. 2021). Hence, we derived a shorter peptide from NaD1, based on its interaction with the V30M TTR protein. Accordingly, both NaD1 and V30M TTR structures were geometrically optimized and docked. Upon docking, the key interacting residues between NaD1 peptide and V30M TTR were elucidated (Fig. 1). It was found that the binding residues viz., C3, K4, T5, E6, S7, S35, K36, I37, L38 and C41 of NaD1 peptide exhibit notable interactions with mutant TTR protein, compared to other residues. To further characterize the binding residues, computational alanine scanning was performed (Fig. 2), in which, the binding residues were replaced by alanine, individually and the resulting changes in NAD1—mutant TTR protein complex in terms of binding energy ($\Delta\Delta G$) were computed. Alanine is a relatively inert amino acid; hence replacing residues and measuring their relative change in binding energy due to alanine substitution, could provide insights into the residual interaction with

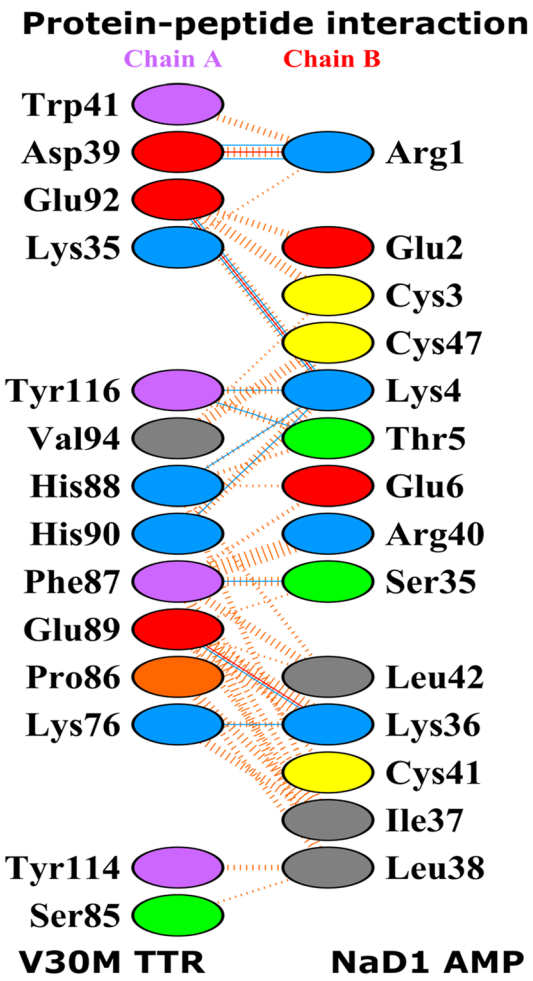


**Fig. 1** Diagram elucidating the interaction between V30M TTR protein and NaD1 AMP peptide. Blue lines depict H-bonds, while the dashed orange lines represent non-bonded contacts and the red lines represent salt-bridges. The sizes of the lines elucidate the intensity of interaction between the residues. The interaction between protein and peptide is predominated by non-bonded contacts with few H-bonds and salt bridges. Also, Binding residues: C3, K4, T5, E6, S7, S35, K36, I37, L38 and C41 of NaD1 peptide exhibit notable interactions with mutant TTR protein, compared to other residues

protein. Thus, post alanine-scanning, the binding residues viz., C3, K4, T5, E6, S7, S35, K36, I37, L38, R40, L42 and C43 of NaD1 peptide were found to exhibit considerable interactions with V30M TTR protein.

Integrating findings from both, the peptide-protein interaction and in silico alanine scanning suggest that the binding residues of NaD1 from residues 3 to 6 (C3, K4, T5, E6) and 35 to 38 (S35, K36, I37, L38) exhibit notable interactions with mutant V30M TTR protein, compared to its other residues. Thus, based on the NaD1 peptide's interaction with mutant TTR, two tetra-peptides with amino acids placed continuously in NaD1 AMP, with residue range 3–6 (CKTE) and 35–38 (SKIL) could be potent therapeutic candidates, in alleviating pathogenic proclivities of V30M TTR protein.

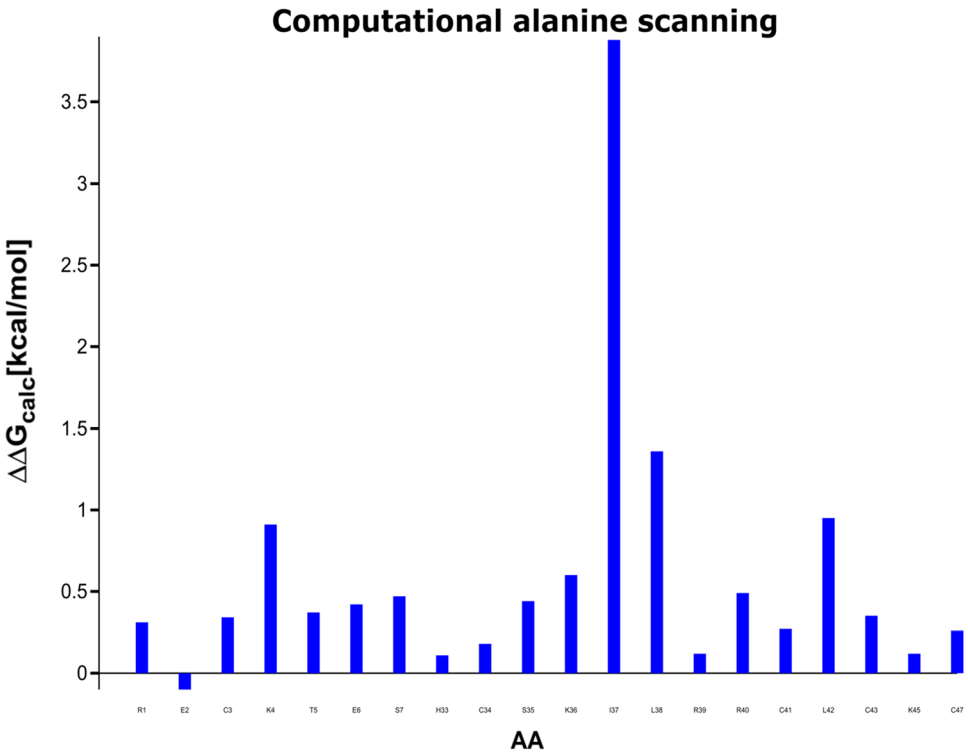


**Fig. 2** Bar graph elucidating the results from Computational Alanine Scanning, the X-axis consists of NaD1's interacting residues with V30M TTR protein that are systematically replaced with alanine, while the Y-axis illustrates the change in free energy in the complex, upon alanine substitution. Binding residues: C3, K4, T5, E6, S7, S35, K36, I37, L38, R40, L42 and C43 of NaD1 peptide were found to exhibit notable energy deviation upon substituted with alanine

## Ascertaining CKTE and SKIL tetra peptide interaction efficacy with V30M TTR

Though the residues in the aforementioned tetra peptide demonstrate notable interactions with mutant V30M TTR, it is imperative in NaD1's structural context, to assess how well these tetra peptides interact with mutant TTR protein independently, when they are sequestered individually from NaD1 AMP.

Accordingly, the tetra peptides: CKTE and SKIL were modelled, optimized geometrically and docked with V30M mutant TTR. While docking, the binding energy between mutant TTR interacting residues and tetra peptides was calculated. Findings indicate that the binding energy of V30M TTR interacting residues with CKTE peptide is comparatively higher (Fig. 3A) than the binding energy of V30M TTR interacting residues with SKIL tetra peptide (Fig. 3B). Thus, the higher binding energy of CKTE with mutant TTR residues suggest that CKTE tetra peptide may indicate stronger interactions with V30M TTR protein, compared to SKIL tetra peptide.

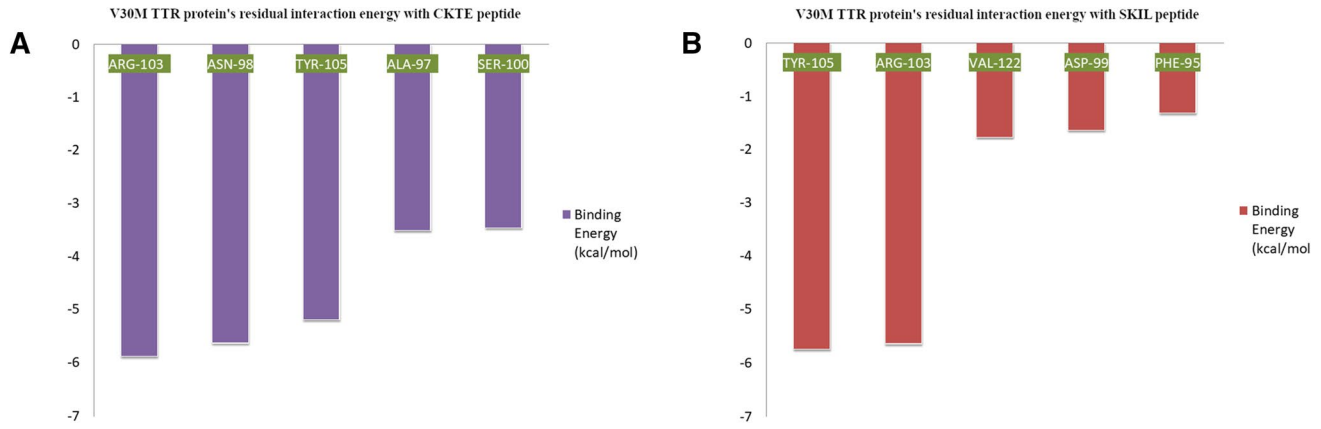


**Fig. 3** Bar graph illustrating mutant V30M TTR protein's residual binding interaction energy with **A** CKTE and **B** SKIL tetra peptides. V30M TTR protein's residual binding interaction energy is relatively higher when it interacts with CKTE peptide, compared to its interaction with SKIL tetra peptide

To further elucidate tetra peptides' association with mutant TTR from a ligand's perspective, both their molecular orbital energies were computed upon docking to V30M TTR protein. The energy difference between the highest occupied molecular orbital (HOMO) and the lowest unoccupied molecular orbital (LUMO) in a ligand after docking, depicts the ligand's reactivity with that protein, wherein, a lower energy gap implicates higher reactivity (Pegu et al. 2017). Upon docking with TTR mutant protein, the HOMO–LUMO energy gap for the CKTE tetra peptide was found to be 1.68 eV (Fig. 4A), while the SKIL tetra peptide exhibited a HOMO–LUMO energy gap of 2.54 eV (Fig. 4B). Thus, the relatively lower energy gap of CKTE tetra peptide suggests its better association and reactivity to V30M TTR protein, compared to SKIL tetra peptide.

Furthermore, steered molecular dynamics (SMD) simulation illustrated the dynamic binding efficacy between the tetra peptides and mutant TTR. SMD simulation is a contrariety protein–ligand interaction analysis to docking, where the ligand is systematically pulled out from the protein, in a controlled simulated environment. Post SMD, protein–ligand binding can be ascertained, based on the time taken for the complete dissociation of the protein and ligand. A ligand having stronger interactions with protein would take a longer duration to be completely pulled out from the complex, and vice versa. Accordingly, the SMD simulation results (Fig. 5) indicate that a relatively longer duration was required to completely pull out the tetra peptide CKTE from its complex with V30M TTR, compared to SKIL. Consequently, SMD simulation

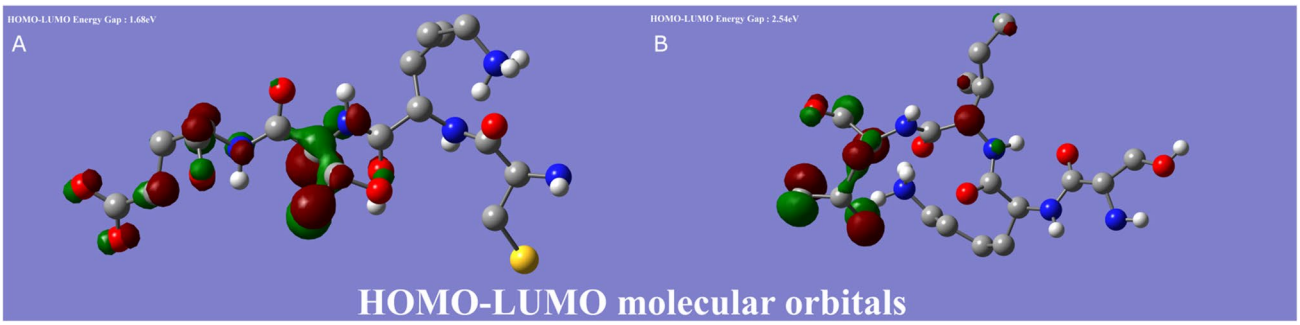


**Fig. 4** Diagram illustrating HOMO–LUMO molecular orbitals of **A** CKTE and **B** SKIL tetra peptides, upon binding to V30M TTR protein. The HOMO–LUMO energy gap for CKTE tetra peptide is relatively lower (indicating a higher reactivity with V30M TTR) compared to the SKIL tetra peptide

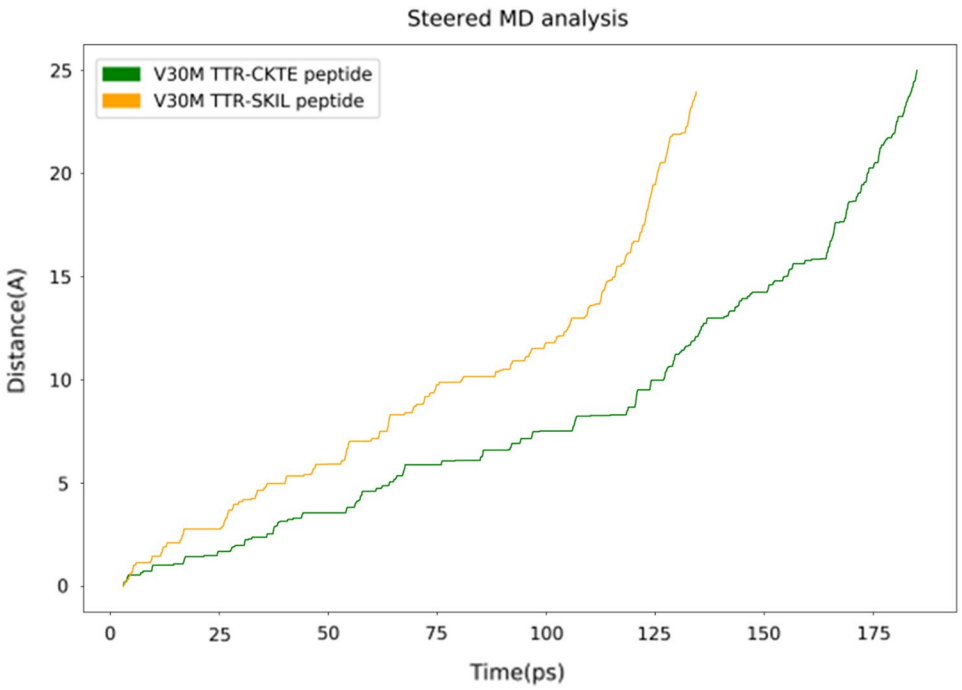


**Fig. 5** Line graph illustrating SMD findings of mutant V30M TTR complex with CKTE and SKIL tetra peptide. A longer duration was observed for the dissociation of CKTE tetra peptide from its complex with V30M TTR protein. This indicates a higher interaction with V30M TTR protein, relative to SKIL tetra peptide

further corroborated the stronger association of CKTE with mutant V30M TTR than SKIL.

Based on the cumulative consistent findings from the aforementioned protein-peptide interaction analyses, it is apparent that the tetra peptides CKTE exhibits a higher interaction with V30M TTR protein, compared to SKIL and more likely, possess the ability to alter the conformational dynamics of mutant V30M TTR protein to steer it away from its pathogenic aggregation propensities.

## Discrete molecular dynamics (DMD) simulation of V30M TTR and its complex with CKTE tetra peptide

Though it was found that the tetra peptide CKTE could considerably interact with V30M TTR compared to SKIL, it is also imperative to analyze its curative potential in notably reorienting the distinct pathogenic conformational dynamics, crucial for V30M TTR's aggregation. To investigate the V30M TTR protein dynamic structural modifications, brought about by CKTE, both V30M TTR mutant protein and its complex with CKTE were subjected to DMD simulation for 100,000 time units. DMD was chosen over the traditional MD simulation since studying the structural dynamics of aggregation-prone proteins typically needs a longer time scale simulation; moreover it is laborious and time-consuming. Furthermore, while classical MD computes the dynamic motion of each and every atom throughout the simulation, DMD's ballistic collision-event-based computation focuses only on the region, where, a conformational change occurs or is likely to occur, which in turn considerably reduces the calculations to be performed. Its fewer computations coupled with coarse-grained implantations make DMD relatively faster when compared to classical MD without leveraging its efficacy (Proctor et al.). To this effect, a study conducted by Yun et al. (2007) reported the use of DMD to effectively elucidate the electrostatic interactions involved in Aβ's oligomer formation. Moreover, Serpa et al. (2021) suggested that DMD simulation can be used to delineate the dynamic conformational changes associated with the oligomer formation of prions. Ding et al. (2012) showed that DMD can better elucidate how SOD1's mutation can engender its misfolding and in turn, effectuate its aggregation. Various other studies have also indicated that DMD can be preferred over classical MD simulation for efficiently delineating the conformational dynamics of amyloidogenic proteins (Buldyrev 2009; Emperador and Orozco 2017; Proctor et al.). Hence, we employed DMD simulation over traditional MD.

Based on the molecular trajectory obtained through DMD simulation, the root-mean-square deviation (RMSD) was calculated for the V30M mutant TTR protein and its complex with CKTE tetra peptide. RMSD computes the average distance moved by atoms with respect to their mean positions thus, elucidating the conformational stability of a protein (Srinivasan and Rajasekaran 2019b; Srinivasan et al. 2021b). Herein, it was found that upon interaction with CKTE tetra peptide, RMSD of V30M TTR protein increased considerably ($p$ value < 0.01), relative to peptide unbound mutant protein (Fig. 6). Hence, suggesting that the pathogenic conformation of mutant TTR is altered upon interacting with CKTE tetra peptide. To further support this perception, the residual flexibility (RMSF) of the protein structures was computed. It was demonstrated that V30M TTR-CKTE complex shows increased residual flexibility ($p$ value < 0.01) for certain amino acids (Fig. 7), thereby alluding to the possibility of structural reorientation, which further reiterates CKTE tetra peptide's ability to re-alter the distinct pathogenic dynamic conformation of V30M TTR.

Since the amyloids are structurally reinforced by beta-sheets and the amyloidogenic proteins tend to misfold into fibrils rich in beta-sheets, targeting and reorienting the residues of beta-sheets of the pathogenic mutant protein might effectively hinder the mutant protein from its aberrant misfolding to amyloid fibrils. Correspondingly, the "beta-sheet breaker" is a crucial metric that is being considered by several studies to evaluate the therapeutic peptides against

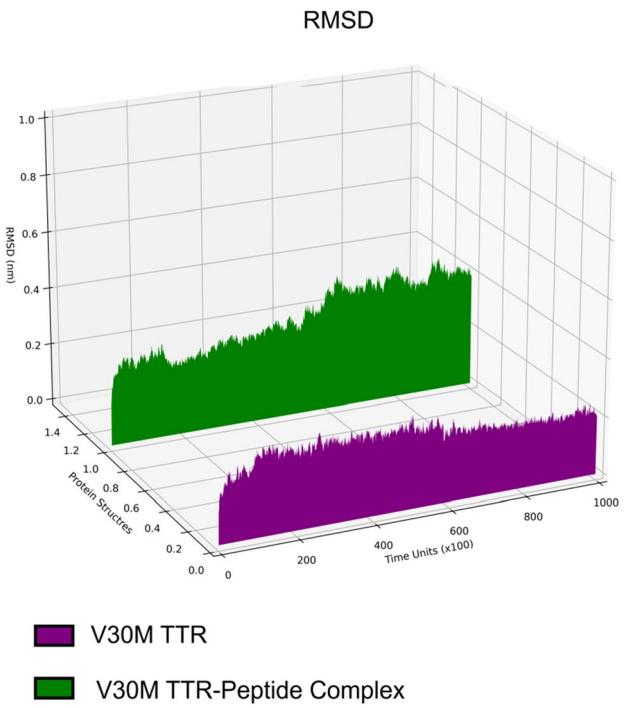


**Fig. 6** 3D line graph illustrating the dynamic change in RMSD of V30M TTR (purple colour) and its complex with CKTE tetra peptide (green colour), observed during DMD simulation. Upon interaction with CKTE tetra peptide, RMSD of V30M TTR protein increased considerably ($p$ value < 0.01), relative to peptide unbound mutant protein

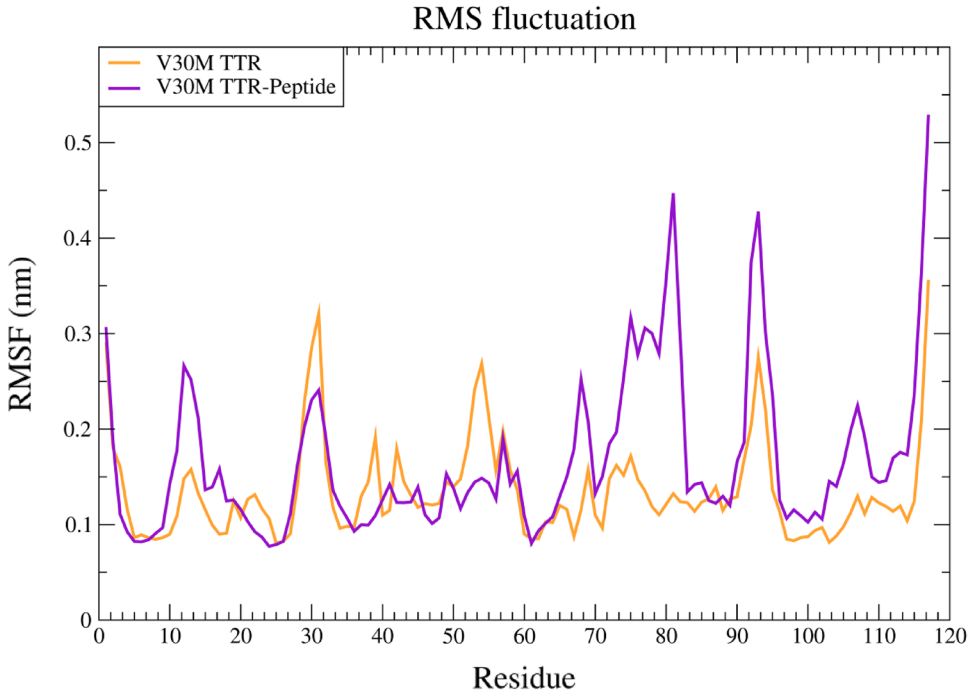


**Fig. 7** Line graph illustrating RMSF of V30M TTR and its complex with CKTE tetra peptide. V30M TTR-CKTE complex shows increased residual flexibility ($p$ value < 0.01) for certain amino acids

amyloid fibrils (Kim et al. 2009; Viet et al. 2011; Lin et al. 2014; Liu et al. 2017; Srinivasan and Rajasekaran 2018). In the present analysis, CKTE's ability to attenuate the beta-sheets of V30M TTR mutant protein was ascertained. Accordingly, the peptide CKTE was able to notably reorient the beta-sheet residue of V30M TTR protein, thereby reducing its beta-sheet content. From Fig. 8, it is apparent that the number of beta-sheet residues decreases considerably ($p$ value < 0.01) upon mutant TTR's interaction with CKTE tetra peptide, relative to peptide unbound V30M TTR. It is further substantiated by the apparent demarcation between their trajectory dataset's running averages. Moreover, while visualizing the binding interface of initial docked V30M TTR-CKTE peptide complex (Supplementary Fig. 1), it was

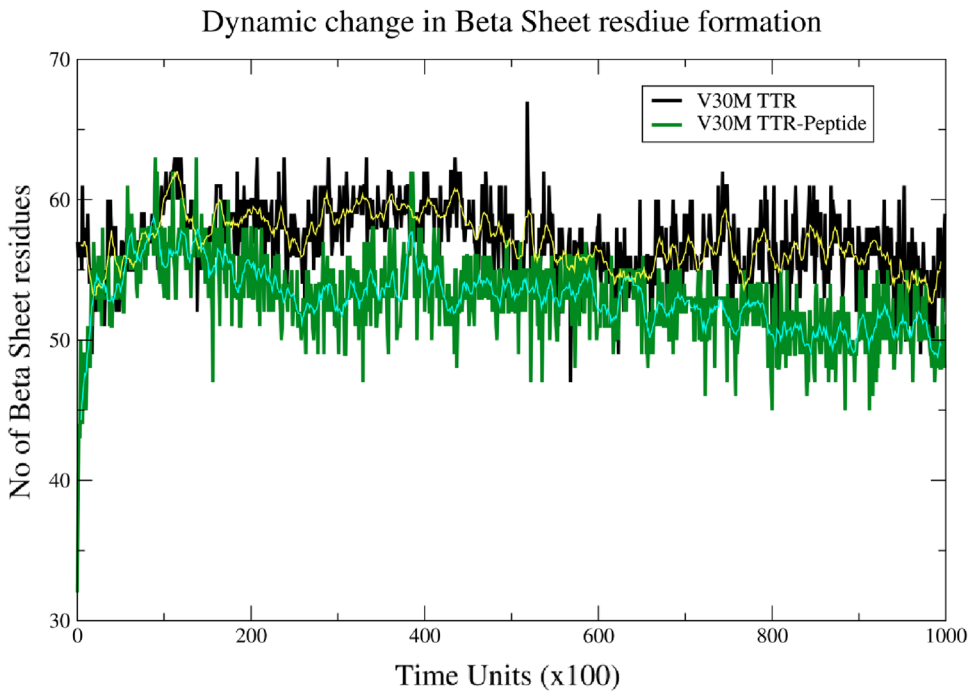


**Fig. 8** Line graph elucidating the dynamic change in beta-sheet residues of V30M TTR and its complex with CKTE tetra peptide. The thin lines depict the moving averages for the corresponding datasets. The number of beta-sheet residues decreases considerably ($p$ value < 0.01) upon mutant TTR's interaction with CKTE tetra peptide

noted that the V30M TTR protein's interacting residues with CKTE peptide, predominantly consists of beta-sheet constituting amino acids. The direct interaction of CKTE tetra peptide with V30M TTR protein's beta-sheet residues could in turn alter the dynamic beta-sheet residue formation of pathogenic V30M TTR protein; this could be the potential causative behind CKTE tetra peptide's "beta-sheet breaker" ability against V30M TTR protein.

Based on the biomolecular trajectory computed during DMD simulation, the covariance of inter-atomic motions was computed for V30M TTR protein and its complex with CKTE tetra peptide. The matrices plotting the covariance of inter-atomic motions for the protein structures (Fig. 9) signifies a distinct change in the pattern of V30M TTR inter-atomic covariance upon its interaction with CKTE tetra peptide. This change in the covariance of inter-atomic motions indicate that the pattern of atomic motion changes considerably upon mutant TTR's binding to CKTE, which further insinuates that CKTE notably alters the distinct pathogenic conformational dynamics of V30M TTR. To further substantiate the notion, a porcupine plot illustrating the principal component, PC1 and PC2 projected motions were plotted based on the molecular trajectories of V30M TTR and its complex with CKTE. Vectors plotted based on the first two principal components PC1 and PC2 (Fig. 10) indicate that the projected motion pattern of V30M TTR changes considerably upon interacting with CKTE. This apparent change in the projected motions of mutant TTR V30M-CKTE complex also substantiate the notion that CKTE could considerably alter the structural dynamics of mutant TTR protein, thereby

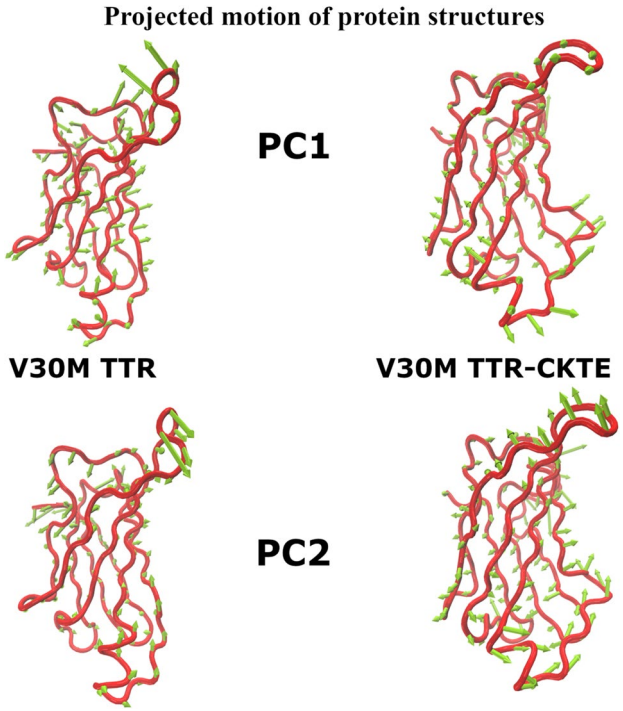


**Fig. 10** Porcupine plots illustrating PC1 and PC2 vector projected motion of V30M TTR and its complex with CKTE peptide. The projected motion pattern of V30M TTR changes considerably upon interacting with CKTE

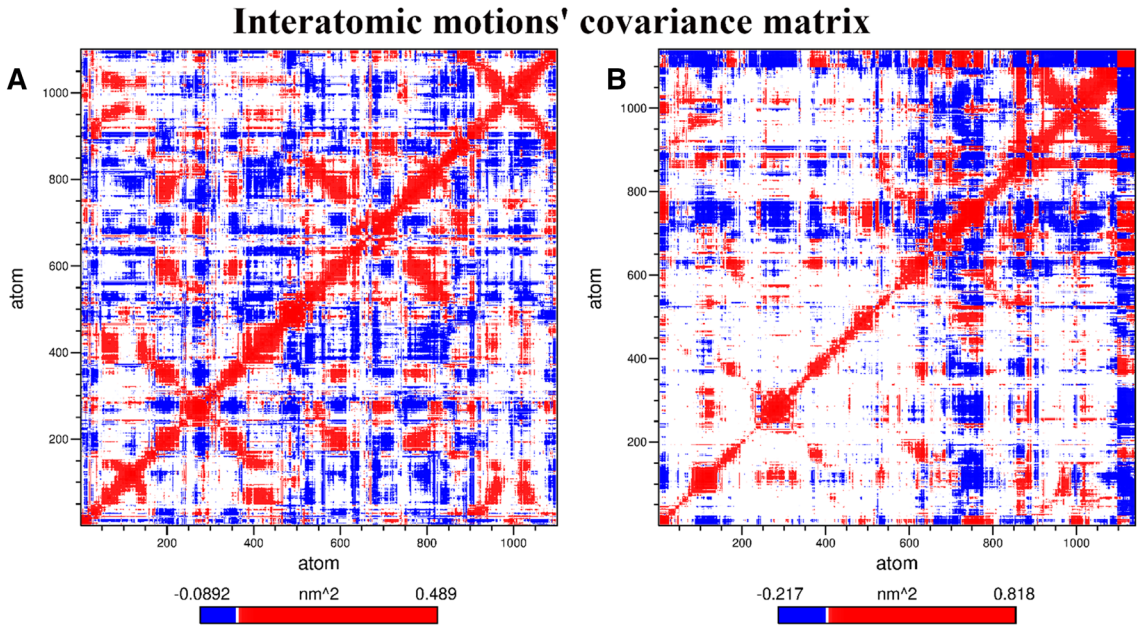


**Fig. 9** Inter-atomic covariance matrix of **A** V30M TTR protein and **B** V30M TTR-CKTE complex. A distinct change in the pattern of V30M TTR inter-atomic covariance upon its interaction with CKTE tetra peptide can be observed

potentially hindering its pathogenic misfolding into amyloid fibrils.

Subsequently, the free energy landscape (FEL) of the protein structures was computed to study the thermodynamically feasible global energy minima states of mutant TTR protein and its complex with CKTE tetra peptide. Herein, the RMSD and the radius of gyration (Rg) of the protein structures were employed as reaction coordinates. Accordingly, the FEL of V30M mutant TTR protein indicate the occurrence of numerous thermodynamically favoured global energy minima states, as illustrated by dark blue contours (Fig. 11A), thereby demonstrating V30M TTR protein's possibility of unprecedented misfolding into amyloid fibrils, wherein any one of the global minima states could aberrantly misfold into amyloid fibrils. However, upon its dynamic association with CKTE tetra peptide, the global energy minima of the complex states reduce notably, as evident from the considerable decrease in the dark blue contours (Fig. 11B). This notable decrease in global energy minima suggests that CKTE tetra peptide's interaction could thermodynamically restrict V30M TTR protein from transforming into one of its pathogenic conformers that fosters amyloidogenic misfolding.

## Normal mode analysis (NMA) of protein structures

To further elucidate the ability of CKTE to alter the pathogenic structural dynamics of V30M TTR protein, NMA simulation was performed on V30M TTR protein and its complex with CKTE tetra peptide. Herein, NMA simulations utilise the classical mechanics to represent atoms as simple sets of tiny harmonic oscillators and computes the biomolecular motions by discerning the atomic amplitudes. NMA is typically used to study a longer timescale conformational transition of biomolecules, which would require larger computational resources and more time if it were studied by traditional molecular simulation procedures. Thus, in the present analysis, we employed NMA to ascertain whether CKTE tetra peptide could regulate V30M TTR pathogenic transitions into amyloid stacks.

Based on NMA simulation, the residual deformation energies were calculated for mutant TTR and its complex with CKTE. Primarily, the deformation energy quantifies the local flexibility of a protein. Herein, the distinct deformation potential of V30M TTR amino acids alters notably upon its binding with CKTE (Fig. 12A and B), thus indicating the potential of CKTE to alter the conformation of mutant TTR, thereby regulating the pathogenic flexibility of its amino acids. Moreover, since the local flexibility of amino acids could determine the molecular basis of protein misfolding (Ferreira and De Felice 2001; Dobson 2003; He et al. 2009; Yaseen et al. 2016), it is safe to infer that CKTE tetra peptide could potentially steer the mutant TTR protein away from its regular misfolding pattern. Also, this change in the residual flexibility pattern between mutant TTR and its CKTE tetra peptide complex is substantiated by the RMSF results of DMD simulation (Fig. 7).

In addition, residual apparent stiffness was computed for the amino acids of V30M TTR protein and its complex with CKTE tetra peptide, where the apparent stiffness is the force experienced among two residues from disconnected oscillators, or in other words, it elucidates the inter-amino acid interactions (Camps et al. 2009). It was found that the residual apparent rigidity is altered notably when mutant TTR protein interacts with CKTE tetra peptide (Fig. 13); further substantiating CKTE peptide's potential to relater the distinct pathogenic conformational dynamics of V30M TTR, thus hindering its amyloidogenic misfolding.

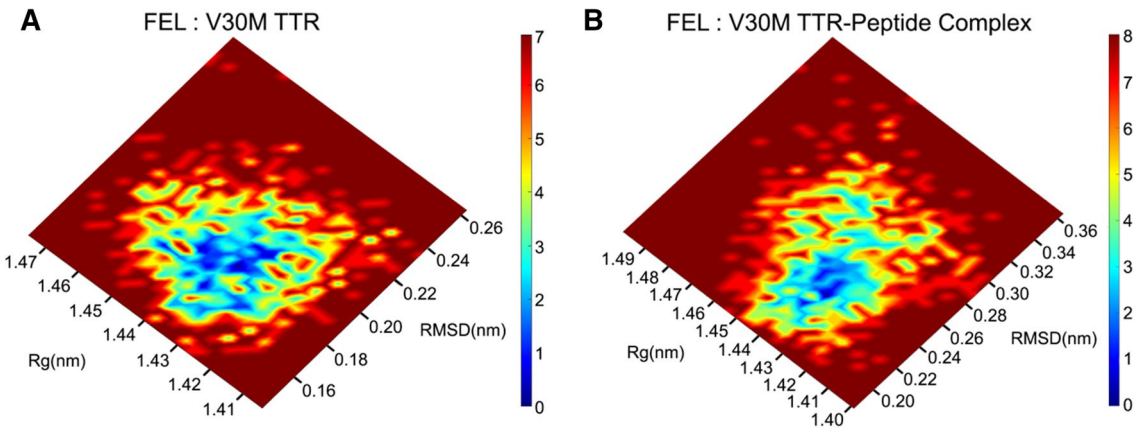


**Fig. 11** FEL diagram of **A** V30M TTR protein and **B** its complex with CKTE tetra peptide. The coloured contours and the colour bar elucidate the energy (kcal/mol) of the conformers. Dark blue regions represent global minima, while light blue and green-coloured regions represent metastable states. Upon V30M TTR's dynamic association with CKTE tetra peptide, the global energy minima of the complex states reduce notably, as evident from the considerable decrease in the dark blue contours

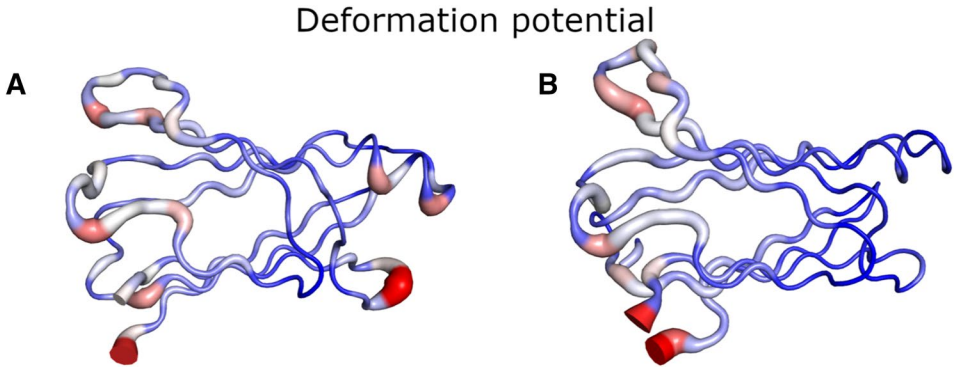


**Fig. 12** Deformation potential diagram of **A** V30M TTR protein and **B** its complex with CKTE tetra peptide. The magnitude of deformation potential is depicted by thickness of tube and colour coded: red (high), white (moderate) and blue (low). Herein, the distinct deformation potential of V30M TTR amino acids alters notably upon its binding with CKTE tetra peptide

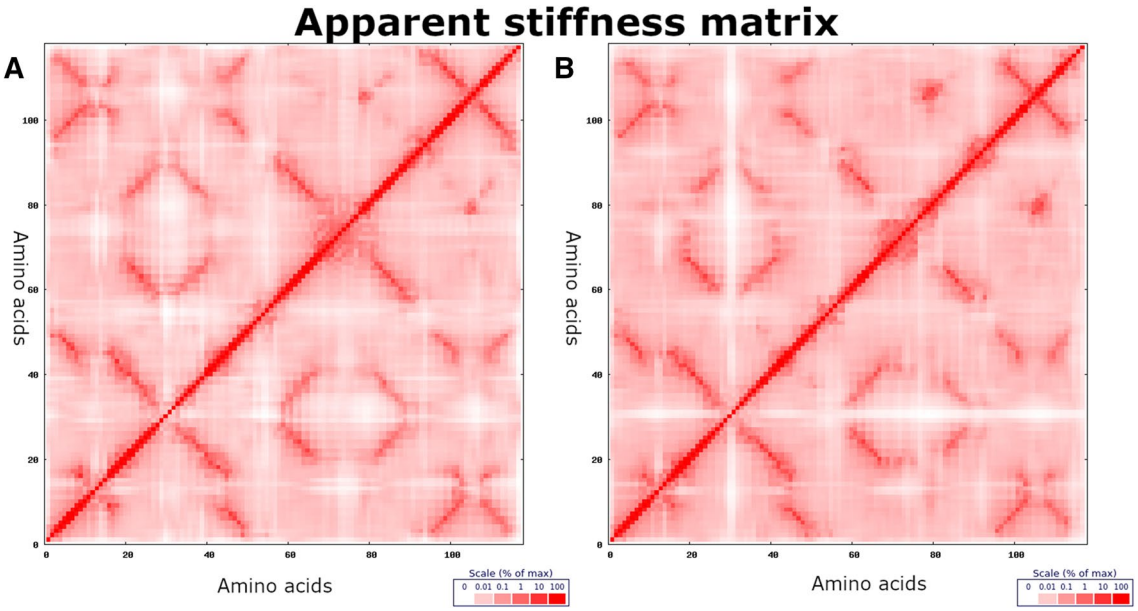


**Fig. 13** Apparent stiffness matrix of **A** V30M TTR protein and **B** its complex with CKTE tetra peptide. The residual apparent rigidity is altered notably when mutant TTR protein interacts with CKTE tetra peptide

## Residual frustration analysis of protein structures

Subsequently, V30M TTR and its complex with CKTE tetra peptide were subjected to residual frustration analysis, which elucidates the likelihood of conformational reorientation of protein structural residues. It computes the likelihood based on a probabilistic model that fits the queried amino-acid's conformation against the list of all possible conformations (Parra et al. 2016). Consequently, the residual frustration analysis (Fig. 14) suggests that due to structural modifications induced by CKTE tetra peptide, the likelihood of conformational reorientation of certain amino acids in mutant TTR protein increases considerably, compared to the pathogenic mutant protein without peptide. Moreover, it is worth mentioning that among the residues that showed an increased likelihood of conformational reorientation are amino acids that correspond to the beta-sheets in mutant V30M TTR. Since the beta-sheets are an integral pathogenic constituent of amyloid fibrils, the results further substantiate the curative potential of CKTE tetra peptide, in conformationally altering the V30M TTR protein from its aggregation propensities.

## Simulated thermal denaturation of protein structures

Simulated thermal denaturation was performed on the protein structures to further examine CKTE's ability to re-alter V30M TTR conformation. In simulated thermal denaturation, the protein is systematically denatured by removing its

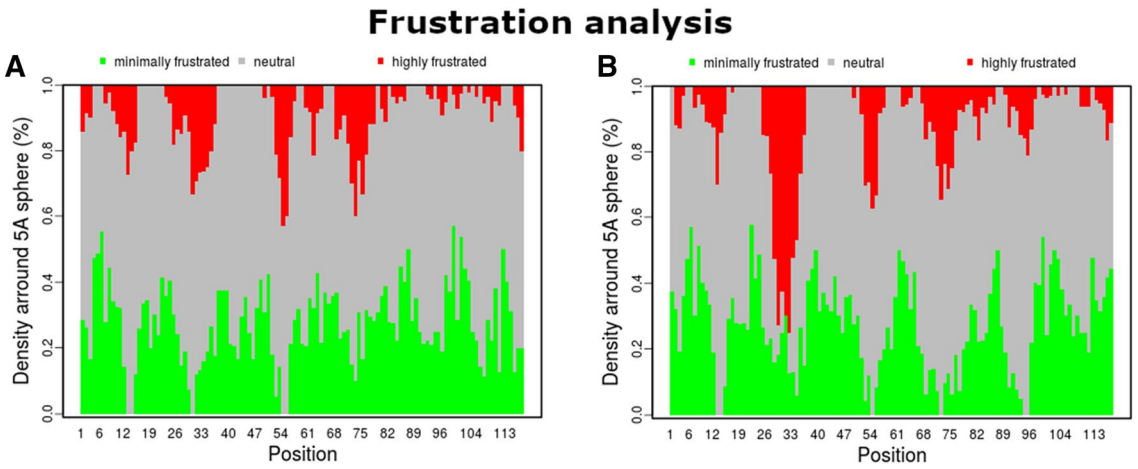


**Fig. 14** Residual frustration analysis graph of **A** V30M TTR protein and **B** its complex with CKTE tetra peptide. Due to structural modifications induced by CKTE tetra peptide, the likelihood of conformational reorientation of certain amino acids in mutant TTR protein increases considerably, compared to the pathogenic mutant protein without peptide

H-bonds, by supplying energy into the system in a simulated environment. Thereby, evaluating the structural integrity of the protein; the higher the energy ingress to denature the protein, the more structurally tenacious and resilient the protein is to conformational reorientation. Accordingly, about − 5.529 kcal/mol energy was required to structurally denature the V30M TTR protein (Fig. 15A), while, about − 4.641 kcal/mol energy was needed to denature V30M TTR-CKTE complex (Fig. 15B). Notably, reduced denaturation energy required by the V30M TTR-CKTE complex suggests that it is more likely susceptible to conformational reorientation, compared to peptide unbound pathogenic V30M TTR protein. This change might be due to the structural modifications on the V30M TTR protein induced by its binding with CKTE tetra peptide.

Hence, based on the consistent findings from various proficient computational analyses, it can be ascertained that the tetra peptide CKTE possesses the therapeutic potential to structurally reorient the pathogenic V30M TTR protein to potentially impede its amyloidogenic misfolding.

## Conclusion

Formulating efficacious analeptics against amyloidogenic disorders has been quite daunting in the pharmaceutical community. While much focus has been given to amyloidogenic disorders such as Alzheimer's and Parkinson's, their equally detrimental counterpart FAP is relatively unheeded. Nevertheless, peptide-based therapeutics has been increasingly postulated to be effective against various detrimental amyloidogenic disorders. Since TTR protein aggregation is one of the main causatives behind FAP and V30M mutant TTR being prevalent in FAP patients, we aimed to formulate the peptide-based analeptics against V30M TTR protein that could effectively hinder its pathogenic misfolding. Accordingly, NaD1 AMP was chosen since it possesses a self-aggregation tendency which could be compliant with aggregation-prone regions of V30M TTR protein. Based on its interaction with mutant TTR protein, two tetra peptides were contrived. Among these, the tetra peptide CKTE showed notable interaction with V30M TTR protein. Based on the consistent findings from various proficient computational analyses including DMD, NMA, residual frustration analysis and simulated thermal denaturation, it is quite apparent that the tetra peptide CKTE possesses the curative potential to notably alter the pathogenic structural dynamics of V30M TTR protein, thus potentially impeding its amyloidogenic misfolding. Hence, we have rationally designed a therapeutic peptide candidate, the tetra peptide CKTE that could attenuate the cytotoxic effects of V30M TTR amyloid aggregates, thereby mitigating the detrimental effects of FAP disorder. Moreover, the tetra peptide CKTE could facilitate future studies towards contriving personalized curatives for FAP patients with aberrant V30M TTR protein.

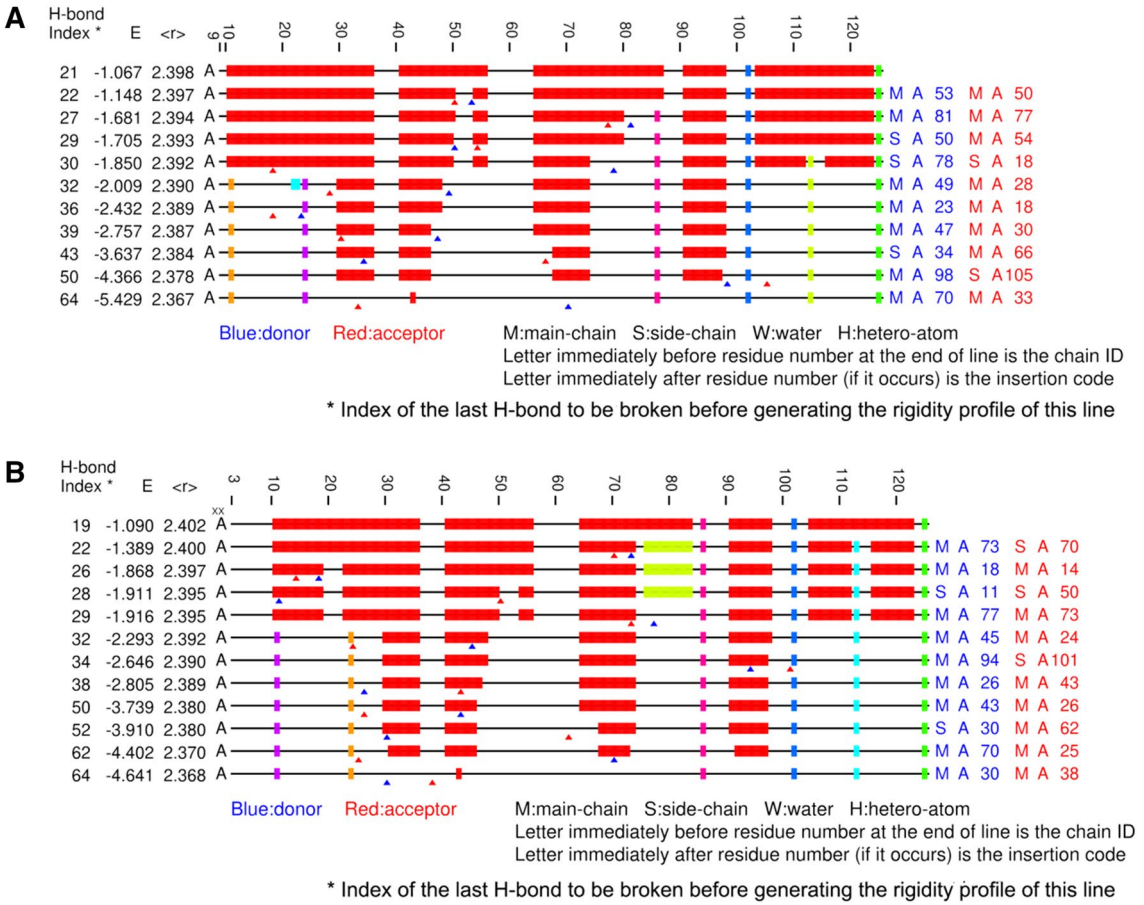


**Fig. 15** Simulated thermal denaturation of **A** V30M TTR and **B** its complex with CKTE tetra peptide. Black lines represent flexible regions while coloured blocks depict rigid regions. Also, the blue triangles depict the H-bond donor and the red triangles represent the H-bond acceptor. Notably, reduced denaturation energy required by the V30M TTR-CKTE complex suggests that it is more likely susceptible to conformational reorientation, compared to peptide unbound pathogenic V30M TTR protein

**Supplementary Information** The online version contains supplementary material available at https://doi.org/10.1007/s13205-023-03646-4.

**Acknowledgements** This study was supported by Provincial Science and Technology Grant of Shanxi Province (20210302124588), Science and Technology Innovation Project of Shanxi province universities (2022L377, 2022L369). Also, we thank the VIT university and ICMR (File no: 5/4-5/Neuro/226/2020/NCD-I) for providing the facilities to carry out this work.

**Data availability** Not applicable.

**Code availability** Not applicable.

## Declarations

**Conflict of interest** The authors declare no competing interest.

**Research involving human participants and/or animals** Not applicable.

**Informed consent** Not applicable.

## References

Adams D (2013) Recent advances in the treatment of familial amyloid polyneuropathy. Ther Adv Neurol Disord 6:129–139. https://doi.org/10.1177/1756285612470192

Andersen HC (1980) Molecular dynamics simulations at constant pressure and/or temperature. J Chem Phys 72:2384–2393. https://doi.org/10.1063/1.439486

Ando Y, Coelho T, Berk JL et al (2013) Guideline of transthyretin-related hereditary amyloidosis for clinicians. Orphanet J Rare Dis 8:31. https://doi.org/10.1186/1750-1172-8-31

Apostolopoulos V, Bojarska J, Chai T-T et al (2021) A global review on short peptides: frontiers and perspectives. Molecules 26:430. https://doi.org/10.3390/molecules26020430

Armiento V, Spanopoulou A, Kapurniotu A (2020) Peptide-based molecular strategies to interfere with protein misfolding, aggregation, and cell degeneration. Angew Chem Int Ed Engl 59:3372–3384. https://doi.org/10.1002/anie.201906908

Arvidsson S, Pilebro B, Westermark P et al (2015) Amyloid cardiomyopathy in hereditary transthyretin V30M amyloidosis—impact of sex and amyloid fibril composition. PLoS ONE 10:e0143456. https://doi.org/10.1371/journal.pone.0143456

Bahar I, Lezon TR, Bakan A, Shrivastava IH (2010) Normal mode analysis of biomolecular structures: functional mechanisms of

membrane proteins. Chem Rev 110:1463–1497. https://doi.org/10.1021/cr900095e
Baig MH, Ahmad K, Saeed M et al (2018) Peptide based therapeutics and their use for the treatment of neurodegenerative and other diseases. Biomed Pharmacother 103:574–581. https://doi.org/10.1016/j.biopha.2018.04.025
Bonaïti B, Olsson M, Hellman U et al (2010) TTR familial amyloid polyneuropathy: does a mitochondrial polymorphism entirely explain the parent-of-origin difference in penetrance? Eur J Hum Genet 18:948–952. https://doi.org/10.1038/ejhg.2010.36
Buldyrev SV (2009) Application of discrete molecular dynamics to protein folding and aggregation. In: Franzese G, Rubi M (eds) Aspects of physical biology. Springer, Berlin, pp 97–131
Camps J, Carrillo O, Emperador A et al (2009) FlexServ: an integrated tool for the analysis of protein flexibility. Bioinformatics 25:1709–1710. https://doi.org/10.1093/bioinformatics/btp304
Carvalho A, Rocha A, Lobato L (2015) Liver transplantation in transthyretin amyloidosis: issues and challenges. Liver Transpl 21:282–292. https://doi.org/10.1002/lt.24058
Cheruvara H, Allen-Baume VL, Kad NM, Mason JM (2015) Intracellular screening of a peptide library to derive a potent peptide inhibitor of α-synuclein aggregation. J Biol Chem 290:7426–7435. https://doi.org/10.1074/jbc.M114.620484
Coelho T, Maia LF, da Silva AM et al (2013) Long-term effects of tafamidis for the treatment of transthyretin familial amyloid polyneuropathy. J Neurol 260:2802–2814. https://doi.org/10.1007/s00415-013-7051-7
Conceição I, González-Duarte A, Obici L et al (2016) "Red-flag" symptom clusters in transthyretin familial amyloid polyneuropathy. J Peripher Nerv Syst 21:5–9. https://doi.org/10.1111/jns.12153
Ding F, Tsao D, Nie H, Dokholyan NV (2008) Ab initio folding of proteins with all-atom discrete molecular dynamics. Structure 16:1010–1018. https://doi.org/10.1016/j.str.2008.03.013
Ding F, Furukawa Y, Nukina N, Dokholyan NV (2012) Local unfolding of Cu, Zn superoxide dismutase monomer determines the morphology of fibrillar aggregates. J Mol Biol 421:548–560. https://doi.org/10.1016/j.jmb.2011.12.029
Dixit A, Verkhivker GM (2011) The energy landscape analysis of cancer mutations in protein kinases. PLoS ONE 6:e26071. https://doi.org/10.1371/journal.pone.0026071
Dobson CM (2003) Protein folding and misfolding. Nature 426:884–890. https://doi.org/10.1038/nature02261
Dokholyan NV, Buldyrev SV, Stanley HE, Shakhnovich EI (1998) Discrete molecular dynamics studies of the folding of a protein-like model. Fold Des 3:577–587. https://doi.org/10.1016/S1359-0278(98)00072-8
Emperador A, Orozco M (2017) Discrete molecular dynamics approach to the study of disordered and aggregating proteins. J Chem Theory Comput 13:1454–1461. https://doi.org/10.1021/acs.jctc.6b01153
Ferreira ST, De Felice FG (2001) PABMB Lecture. Protein dynamics, folding and misfolding: from basic physical chemistry to human conformational diseases. FEBS Lett 498:129–134. https://doi.org/10.1016/s0014-5793(01)02491-7
Gertz MA, Benson MD, Dyck PJ et al (2015) Diagnosis, prognosis, and therapy of transthyretin amyloidosis. J Am Coll Cardiol 66:2451–2466. https://doi.org/10.1016/j.jacc.2015.09.075
Go N, Noguti T, Nishikawa T (1983) Dynamics of a small globular protein in terms of low-frequency vibrational modes. Proc Natl Acad Sci USA 80:3696–3700. https://doi.org/10.1073/pnas.80.12.3696
Hassan M, Shahzadi S, Seo SY et al (2018) Molecular docking and dynamic simulation of AZD3293 and solanezumab effects against BACE1 to treat Alzheimer's disease. Front Comput Neurosci 12:34. https://doi.org/10.3389/fncom.2018.00034
Hayes BME, Bleackley MR, Anderson MA, van der Weerden NL (2018) The plant defensin NaD1 enters the cytoplasm of Candida Albicans via Endocytosis. J Fungi (basel) 4:E20. https://doi.org/10.3390/jof4010020
He B, Wang K, Liu Y et al (2009) Predicting intrinsic disorder in proteins: an overview. Cell Res 19:929–949. https://doi.org/10.1038/cr.2009.87
Hinsen K (1998) Analysis of domain motions by approximate normal mode calculations. Proteins 33:417–429. https://doi.org/10.1002/(sici)1097-0134(19981115)33:3%3c417::aid-prot10%3e3.0.co;2-8
Jakubowski JM, Orr AA, Le DA, Tamamis P (2020) Interactions between curcumin derivatives and amyloid-β fibrils: insights from molecular dynamics simulations. J Chem Inf Model 60:289–305. https://doi.org/10.1021/acs.jcim.9b00561
Järvå M, Lay FT, Phan TK et al (2018) X-ray structure of a carpet-like antimicrobial defensin–phospholipid membrane disruption complex. Nat Commun 9:1962. https://doi.org/10.1038/s41467-018-04434-y
Kim YS, Lim D, Kim JY et al (2009) β-Sheet-breaking peptides inhibit the fibrillation of human α-synuclein. Biochem Biophys Res Commun 387:682–687. https://doi.org/10.1016/j.bbrc.2009.07.083
Kozakov D, Hall DR, Xia B et al (2017) The ClusPro web server for protein–protein docking. Nat Protoc 12:255–278. https://doi.org/10.1038/nprot.2016.169
La Manna S, Di Natale C, Florio D, Marasco D (2018) Peptides as therapeutic agents for inflammatory-related diseases. IJMS 19:2714. https://doi.org/10.3390/ijms19092714
Lay FT, Schirra HJ, Scanlon MJ et al (2003) The three-dimensional solution structure of NaD1, a new floral defensin from Nicotiana alata and its application to a homology model of the crop defense protein alfAFP. J Mol Biol 325:175–188. https://doi.org/10.1016/s0022-2836(02)01103-8
Lazaridis T, Karplus M (1999) Effective energy function for proteins in solution. Proteins 35:133–152. https://doi.org/10.1002/(SICI)1097-0134(19990501)35:2%3c133::AID-PROT1%3e3.0.CO;2-N
Lemkul JA, Bevan DR (2012) The role of molecular simulations in the development of inhibitors of amyloid β-peptide aggregation for the treatment of Alzheimer's disease. ACS Chem Neurosci 3:845–856. https://doi.org/10.1021/cn300091a
Levitt M, Sander C, Stern PS (1985) Protein normal-mode dynamics: trypsin inhibitor, crambin, ribonuclease and lysozyme. J Mol Biol 181:423–447. https://doi.org/10.1016/0022-2836(85)90230-x
Lin L, Bo X, Tan Y et al (2014) Feasibility of β-sheet breaker peptide-H102 treatment for Alzheimer's disease based on β-amyloid hypothesis. PLoS One 9:e112052. https://doi.org/10.1371/journal.pone.0112052
Liu W, Sun F, Wan M et al (2017) β-sheet breaker peptide-HPYD for the treatment of Alzheimer's disease: primary studies on behavioral test and transcriptional profiling. Front Pharmacol 8:969. https://doi.org/10.3389/fphar.2017.00969
Parra RG, Schafer NP, Radusky LG et al (2016) Protein Frustratometer 2: a tool to localize energetic frustration in protein molecules, now with electrostatics. Nucleic Acids Res 44:W356–W360. https://doi.org/10.1093/nar/gkw304
Pegu D, Deb J, Van Alsenoy C, Sarkar U (2017) Theoretical investigation of electronic, vibrational, and nonlinear optical properties of 4-fluoro-4-hydroxybenzophenone. Spectrosc Lett 50:232–243. https://doi.org/10.1080/00387010.2017.1308381
Proctor EA, Ding F, Dokholyan NV (2011) Discrete molecular dynamics. Comput Mol Sci 1:80–92. https://doi.org/10.1002/wcms.4. (**Wiley Interdisciplinary Reviews**)
Rader AJ, Hespenheide BM, Kuhn LA, Thorpe MF (2002) Protein unfolding: rigidity lost. Proc Natl Acad Sci USA 99:3540–3545. https://doi.org/10.1073/pnas.062492699
Rodrigues CH, Pires DE, Ascher DB (2018) DynaMut: predicting the impact of mutations on protein conformation, flexibility and stability. Nucleic Acids Res 46:W350–W355. https://doi.org/10.1093/nar/gky300

Rowczenio DM, Noor I, Gillmore JD et al (2014) Online registry for mutations in hereditary amyloidosis including nomenclature recommendations. Hum Mutat 35:E2403-2412. https://doi.org/10.1002/humu.22619

Saelices L, Johnson LM, Liang WY et al (2015) Uncovering the mechanism of aggregation of human transthyretin. J Biol Chem 290:28932–28943. https://doi.org/10.1074/jbc.M115.659912

Santos D, Coelho T, Alves-Ferreira M et al (2015) The hidden story behind gender differences in familial amyloid polyneuropathy (FAP) ATTRV30M. Orphanet J Rare Dis 10:O4. https://doi.org/10.1186/1750-1172-10-S1-O4

Saraiva MJ (1995) Transthyretin mutations in health and disease. Hum Mutat 5:191–196. https://doi.org/10.1002/humu.1380050302

Sekijima Y (2015) Transthyretin (ATTR) amyloidosis: clinical spectrum, molecular pathogenesis and disease-modifying treatments. J Neurol Neurosurg Psychiatry 86:1036–1043. https://doi.org/10.1136/jnnp-2014-308724

Sekijima Y, Ueda M, Koike H et al (2018) Diagnosis and management of transthyretin familial amyloid polyneuropathy in Japan: red-flag symptom clusters and treatment algorithm. Orphanet J Rare Dis 13:6. https://doi.org/10.1186/s13023-017-0726-x

Serpa JJ, Popov KI, Petrotchenko EV et al (2021) Structure of prion β-oligomers as determined by short-distance crosslinking constraint-guided discrete molecular dynamics simulations. Proteomics 21:e2000298. https://doi.org/10.1002/pmic.202000298

Sharma M, Khan S, Rahman S, Singh LR (2019) The extracellular protein, transthyretin is an oxidative stress biomarker. Front Physiol 10:5. https://doi.org/10.3389/fphys.2019.00005

Shirvanyants D, Ding F, Tsao D et al (2012) Discrete molecular dynamics: an efficient and versatile simulation method for fine protein characterization. J Phys Chem B 116:8375–8382. https://doi.org/10.1021/jp2114576

Srinivasan E, Rajasekaran R (2017) Computational simulation analysis on human SOD1 mutant (H80R) exposes the structural destabilization and the deviation of Zn binding that directs familial amyotrophic lateral sclerosis. J Biomol Struct Dyn 35:2645–2653. https://doi.org/10.1080/07391102.2016.1227723

Srinivasan E, Rajasekaran R (2018) Comparative binding of kaempferol and kaempferide on inhibiting the aggregate formation of mutant (G85R) SOD1 protein in familial amyotrophic lateral sclerosis: a quantum chemical and molecular mechanics study: a quantum chemical and molecular mechanics study. BioFactors 44:431–442. https://doi.org/10.1002/biof.1441

Srinivasan E, Rajasekaran R (2019a) Rational design of linear tripeptides against the aggregation of human mutant SOD1 protein causing amyotrophic lateral sclerosis. J Neurol Sci 405:116425. https://doi.org/10.1016/j.jns.2019.116425

Srinivasan E, Rajasekaran R (2019b) Molecular binding response of naringin and naringenin to H46R mutant SOD1 protein in combating protein aggregation using density functional theory and discrete molecular dynamics. Prog Biophys Mol Biol 145:40–51. https://doi.org/10.1016/j.pbiomolbio.2018.12.003

Srinivasan E, Natarajan N, Rajasekaran R (2020) TTRMDB: a database for structural and functional analysis on the impact of SNPs over transthyretin (TTR) using bioinformatic tools. Comput Biol Chem 87:107290. https://doi.org/10.1016/j.compbiolchem.2020.107290

Srinivasan E, Chandrasekhar G, Chandrasekar P et al (2021a) Decoding conformational imprint of convoluted molecular interactions between prenylflavonoids and aggregated amyloid-Beta42 peptide causing Alzheimer's disease. Front Chem 9:753146. https://doi.org/10.3389/fchem.2021.753146

Srinivasan E, Chandrasekhar G, Chandrasekar P et al (2021b) Decoding conformational imprint of convoluted molecular interactions between prenylflavonoids and aggregated amyloid-Beta42 peptide causing Alzheimer's disease. Front Chem 9:753146. https://doi.org/10.3389/fchem.2021.753146

Srinivasan E, Chandrasekhar G, Rajasekaran R (2022) Probing the polyphenolic flavonoid, morin as a highly efficacious inhibitor against amyloid(A4V) mutant SOD1 in fatal amyotrophic lateral sclerosis. Arch Biochem Biophys 727:109318. https://doi.org/10.1016/j.abb.2022.109318

Stewart JJP (2007) Optimization of parameters for semiempirical methods V: modification of NDDO approximations and application to 70 elements. J Mol Model 13:1173–1213. https://doi.org/10.1007/s00894-007-0233-4

Tang Y, Zhang D, Gong X, Zheng J (2022) Repurposing of intestinal defensins as multi-target, dual-function amyloid inhibitors via cross-seeding. Chem Sci 13:7143–7156. https://doi.org/10.1039/d2sc01447e

Vajda S, Yueh C, Beglov D et al (2017) New additions to the C lus P ro server motivated by CAPRI. Proteins 85:435–444. https://doi.org/10.1002/prot.25219

Van Der Spoel D, Lindahl E, Hess B et al (2005) GROMACS: fast, flexible, and free. J Comput Chem 26:1701–1718. https://doi.org/10.1002/jcc.20291

van der Weerden NL, Lay FT, Anderson MA (2008) The plant defensin, NaD1, enters the cytoplasm of Fusarium oxysporum hyphae. J Biol Chem 283:14445–14452. https://doi.org/10.1074/jbc.M709867200

van der Weerden NL, Hancock REW, Anderson MA (2010) Permeabilization of fungal hyphae by the plant defensin NaD1 occurs through a cell wall-dependent process. J Biol Chem 285:37513–37520. https://doi.org/10.1074/jbc.M110.134882

Viet MH, Ngo ST, Lam NS, Li MS (2011) Inhibition of aggregation of amyloid peptides by beta-sheet breaker peptides and their binding affinity. J Phys Chem B 115:7433–7446. https://doi.org/10.1021/jp1116728

Walensky LD, Bird GH (2014) Hydrocarbon-stapled peptides: principles, practice, and progress: miniperspective. J Med Chem 57:6275–6288. https://doi.org/10.1021/jm4011675

Wang F, Zhou X-L, Yang Q-G et al (2011) A peptide that binds specifically to the β-amyloid of Alzheimer's disease: selection and assessment of anti-β-amyloid neurotoxic effects. PLoS ONE 6:e27649. https://doi.org/10.1371/journal.pone.0027649

Wang L, Wang N, Zhang W et al (2022) Therapeutic peptides: current applications and future directions. Sig Transduct Target Ther 7:48. https://doi.org/10.1038/s41392-022-00904-4

Weng G, Wang E, Wang Z et al (2019) HawkDock: a web server to predict and analyze the protein–protein complex based on computational docking and MM/GBSA. Nucleic Acids Res 47:W322–W330. https://doi.org/10.1093/nar/gkz397

Werle M, Bernkop-Schnürch A (2006) Strategies to improve plasma half life time of peptide and protein drugs. Amino Acids 30:351–367. https://doi.org/10.1007/s00726-005-0289-3

Yaseen A, Nijim M, Williams B et al (2016) FLEXc: protein flexibility prediction using context-based statistics, predicted structural features, and sequence information. BMC Bioinform 17:281. https://doi.org/10.1186/s12859-016-1117-3

Yun S, Urbanc B, Cruz L et al (2007) Role of electrostatic interactions in amyloid β-protein (Aβ) oligomer formation: a discrete molecular dynamics study. Biophys J 92:4064–4077. https://doi.org/10.1529/biophysj.106.097766

Zhang Y, Liu Y, Tang Y et al (2021) Antimicrobial α-defensins as multi-target inhibitors against amyloid formation and microbial infection. Chem Sci 12:9124–9139. https://doi.org/10.1039/d1sc01133b